

Mechanical Characteristics of a Tool Steel Layer Deposited by Using Direct Energy Deposition

Gyeong Yun Baek¹, Gwang Yong Shin², Eun Mi Lee¹, Do Sik Shim^{3,*}, Ki Yong Lee²,
Hi-Seak Yoon¹, and Myoung Ho Kim²

¹Department of Mechanical Engineering, Chonnam National University, Gwangju 61186, Republic of Korea

²Green Manufacturing Process Group, KITECH, Gwangju 61007, Republic of Korea

³Division of Mechanical Engineering, Korea Maritime and Ocean University, Busan 49112, Republic of Korea

(received date: 28 June 2016 / accepted date: 6 September 2016)

This study focuses on the mechanical characteristics of layered tool steel deposited using direct energy deposition (DED) technology. In the DED technique, a laser beam bonds injected metal powder and a thin layer of substrate via melting. In this study, AISI D2 substrate was hardfaced with AISI H13 and M2 metal powders for mechanical testing. The mechanical and metallurgical characteristics of each specimen were investigated via microstructure observation and hardness, wear, and impact tests. The obtained characteristics were compared with those of heat-treated tool steel. The microstructures of the H13- and M2-deposited specimens show fine cellular-dendrite solidification structures due to melting and subsequent rapid cooling. Moreover, the cellular grains of the deposited M2 layer were smaller than those of the H13 structure. The hardness and wear resistance were most improved in the M2-deposited specimen, yet the H13-deposited specimen had higher fracture toughness than the M2-deposited specimen and heat-treated D2.

Keywords: metal, surface modification, powder processing, toughness, wear

1. INTRODUCTION

As energy savings through the weight reduction of vehicles becomes an issue around the world, many researchers have focused on the use of lightweight materials such as advanced high-strength steels (AHSS). However, conventional tool steel for fabricating AHSS has problems of low durability such as low wear resistance and toughness. For this reason, in industrial fields, tool steel is either prehardened by a heat treatment or surface-coated by chemical vapor deposition (CVD) or physical vapor deposition (PVD) before practical usage. However, the conventional methods for enhancing tool steel life have limitations owing to its application in a harsh manufacturing environment.

Recently, additive manufacturing (AM) has become an attractive and rapidly developing solution in diverse industrial applications. Among AM technologies, directed energy deposition (DED) technology, which is capable of achieving three-dimensional molding with the purpose of diverse shaping and local strengthening of metallic surfaces, is receiving much attention. DED technology can be used for hardfacing the surface of tool steel and repairing damaged products as it exhibits a superior refined microstructure and strong fusion

bonding between the substrate and metal powder. Additionally, as the heat affected zone (HAZ), which leads to softening of the material, can be minimized, it is expected to replace conventional methods such as arc welding [1].

In particular, DED has been a popular method among die/mold industries for improving surface properties. Many studies with the purpose of improving the tool life have reported on the improvement of wear resistance by depositing a thin layer of high performance metal powder on the target materials. Park and Ahn [2] improved wear resistance by depositing Stellite6 and NOREM02 metal powder onto a hot forged die, and Wang *et al.* [3] coated the surface of tool steel with CPM metal powder with a high vanadium content and compared the characteristics of the wear behavior. Park *et al.* [4] deposited D2 and H13 metal powder onto D2 tool steel, which they then heat treated; subsequently, they observed the change in hardness and microstructure caused by the post-heat treatment. Pleterski *et al.* [5] clad D2 material under pre-heated and cryogenic conditions and checked its punching life by applying it to an actual blanking process. Alternatively, studies have also been performed on the change in mechanical properties depending on powder characteristics [6] and the prediction of the clad layer fatigue life [7]. Moon *et al.* [8] investigated the wear resistance and the friction coefficient of a deposited layer by using Fe-Cr and Fe-Ni powders and

*Corresponding author: think@kmou.ac.kr

compared with the H13 tool steel. Kim *et al.* [9] characterized the microstructures and corrosion properties, including stress corrosion cracking, of welded SUS 304 stainless steel surface-melted by a laser beam.

However, in the case of tool steel that undergoes the cold pressing process for high strength steel products, high toughness is required in addition to high hardness and high wear resistance. Nevertheless, studies that can evaluate such comprehensive durability of hardfaced tool steel have been insufficient. Accordingly, in this study, AISI D2 metal, which is widely used in cold press processes, was hardfaced by depositing H13 tool steel and M2 high-speed tool steel by using DED technology, and the mechanical properties of these surface coatings were investigated. The wear resistance of the deposited metal layer was analyzed, and a Charpy impact test, which can qualitatively evaluate the fracture toughness, was performed. This study also discusses improvement in mechanical properties through hardfacing of H13 and M2 powders by comparing with conventional heat-treated tool steel.

2. EXPERIMENTAL PROCEDURE

2.1. DED Processing Conditions

The laser-assisted metal lamination equipment used for our

research—a direct metal tooling (DMT) MX3 device developed by Insstek (South Korea) Co., Ltd.—is shown in Fig. 1(a). The device consists of a 4-kW CO₂ laser that serves as the heat source, a numerical control system (including an industrial operating computer), MX-CAM software, a five-axis NC machine tool, and a powder feeding system that consists of three hoppers and a coaxial powder nozzle. Figure 1(b) shows a multi-layer deposited along a “zigzag” path, wherein the track follows back-and-forth motions in a fixed direction. The beam spot diameter is 1.0 mm with a top-hat intensity distribution. Thus, overlapping tracks were applied with a pitch of 0.5 mm. The experiments were performed with argon as the shielding gas for the protection of the workpiece against oxidation as well as the carrier gas for the injected powder. The processing head, which was equipped with a coaxial supply of powder, was integrated with the optical system to feed the powder coaxially with the laser beam on the substrate surface, placed 9 mm from the nozzle tip. The optimum processing conditions obtained from preliminary experiments are summarized in Table 1.

2.2. Materials

For the experimental studies, AISI D2 material was used as the substrate. D2 is tool steel widely used as a cold press

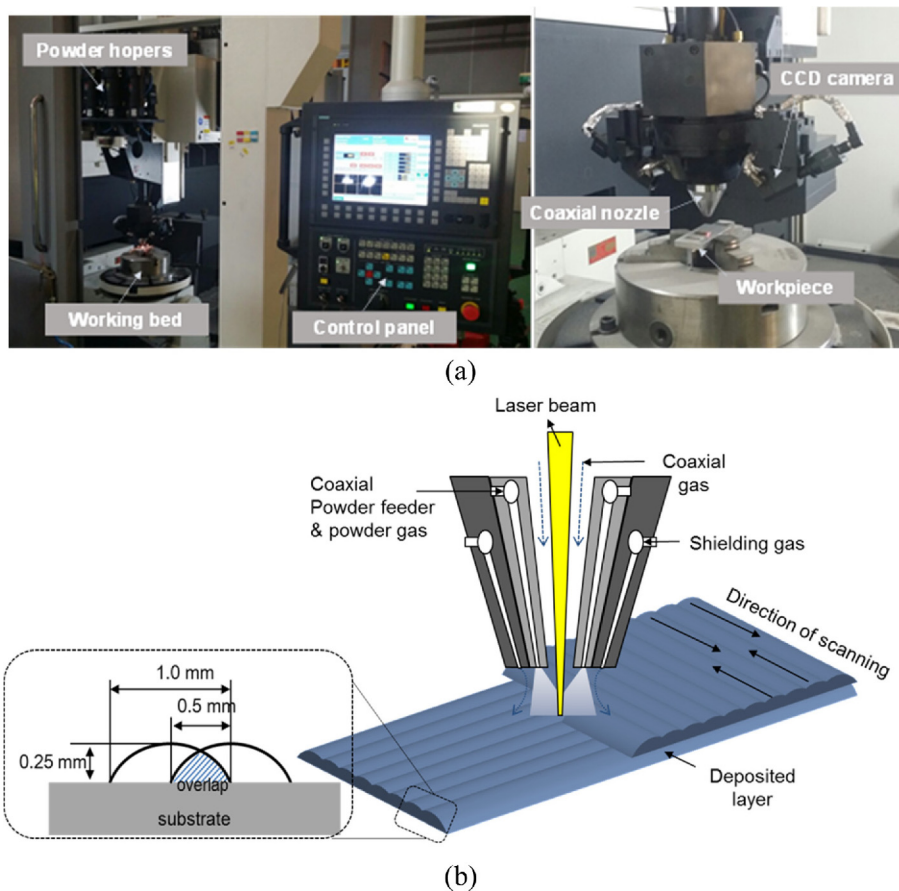


Fig. 1. (a) Schematic diagram of the scanning procedure for the multi-layer deposition and (b) photographs of DED machine.

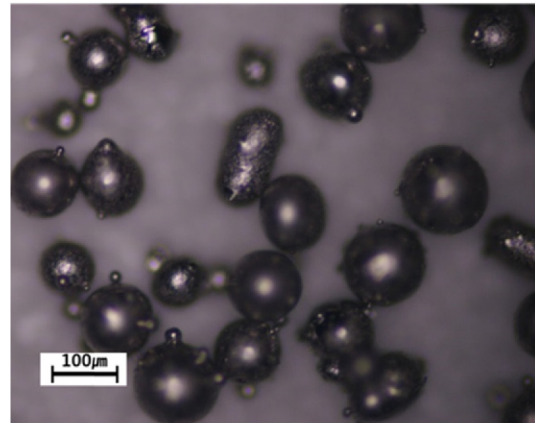
Table 1. Parameters for DED processing

Laser beam power (W)	900
Slicing layer height (mm)	0.25
Overlap width (mm)	0.5
Powder flow rate (g/min)	5
Laser traverse speed (mm/min)	850
Powder gas (l/min)	2.5
Coaxial gas (l/min)	8.0

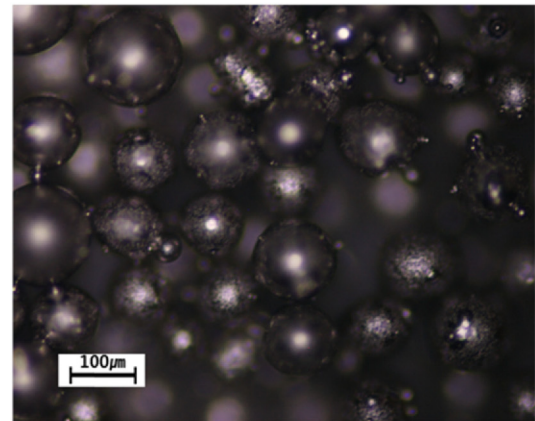
die and mold material because it combines appropriate wear resistance with toughness while also possessing good machinability. Moreover, as D2 is characterized by very high carbon and chrome contents, it has been used for practical purposes after being hardened through the heat treatment of quenching and tempering [10]. The mechanical properties of the deposited tool steels were compared with the heat-treated D2; the reference D2 steel was austenitized at 1293 K for 180 min in a vacuum and quenched to room temperature and then tempered at 823 K for 270 min. H13 and M2 with spherical particle morphologies and average particle sizes of approximately 120 μm were applied as the depositing powder materials. Figure 2 shows the morphology of the M2 and H13 powders (supplied by Carpenter Co.). H13 is highly utilizable as a hot forged mold material for the purpose of repairing cracks and reinforcing thermal fatigue resistance as it has superior high-temperature wear characteristics [11]. M2 is a molybdenum-based high-speed tool steel that is used for general tools, such as cold forged tools or molds and parts for a high-speed press, which require toughness, as its toughness is also good because it contains tungsten [12,13]. Table 2 shows the chemical composition of each material.

2.3. Mechanical Tests

For the observation of the microstructure of the deposited layer, A3, 1- μm diamond paste, and 0.5- μm diamond paste were used to polish each sample after perpendicularly cutting the specimens. The substrate was etched for several seconds by using the etchant, Nital (Nitric acid 1% + ethyl alcohol), after a mirror-like polishing, and the microstructure was observed using a field emission scanning electron microscope (FE-SEM, JEOL Ltd, 7100f). As the corrosion resistances of the deposited materials differ from each other, they were etched using different etching solutions and conditions. The deposited H13 layer was etched for 5 to 10 sec by using Nital (Nitric acid 3% + ethyl alcohol), and the deposited M2 layer, which has high corrosion resistance, was etched for 30 to 50 sec by



(a)



(b)

Fig. 2. Photographs of (a) AISI H13 and (b) AISI M2 powders.

using aqua regia (Nitric acid and Hydrogen chloride with a molar ratio of 1:3, respectively).

Depth-sensing micro-indentation tests were performed using an AAV-502 (Akashi, Japan) microhardness tester. The microhardness of the deposited layer was measured vertically and horizontally. The value of hardness at each position was obtained by calculating the area of the indentation mark made by applying a load of 980.7 mN for 10 sec by using a penetrator.

To compare the wear characteristics, wear specimens were prepared by depositing metal powder onto a cylindrical specimen, as shown in Fig. 3(a). A ball-on-disk wear tester (R&B Inc.) was used, and the ball was set to be rotated on the top surface of the specimen for 10 min with the conditions of a 147.1-N (15 kgf) loading and a 10.49-rad/s (100 rpm) ball

Table 2. Chemical compositions of materials (remaining fraction is Fe) (wt%)

Metal	C	Si	Mn	P	S	Ni	Cr	Mo	Cu	V	W
D2	1.56	0.241	0.25	0.025	0.001	0.175	11.312	0.829	0.141	0.248	-
H13	0.4	0.98	0.45	0.015	0.005	-	5.2	1.53	-	1.05	-
M2	0.803	0.16	0.29	0.018	0.013	0.07	3.98	4.84	-	2.03	5.84

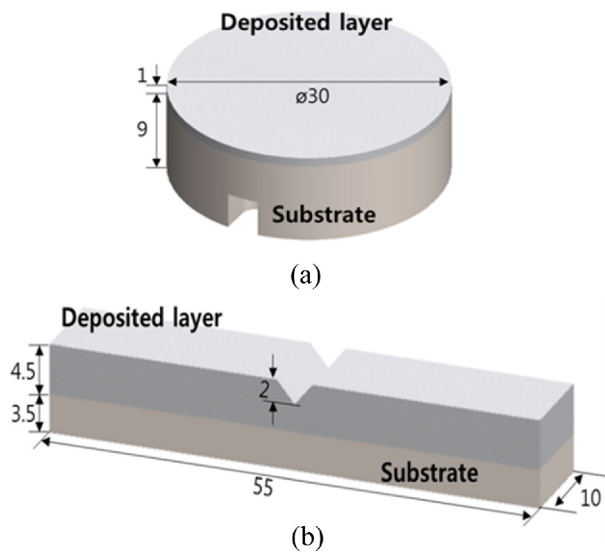


Fig. 3. Schematic representation of specimens for (a) wear test and (b) Charpy impact Test (unit: mm).

speed. To evaluate the wear resistance of each specimen, the weight loss, width of the wear track, and friction coefficient were measured. The weight loss is measured by the change in weight before and after the test, and the friction coefficient was calculated via $\text{friction coefficient} = (\text{load} \times \text{distance}) /$

(worn volume). The width of the wear track was measured using a toolmaker's microscope.

To evaluate toughness, which is the resistance against fracture, a Charpy impact test was performed. The specimen for the impact test was prepared from an 8 mm × 10 mm × 55 mm block with a 4.5-mm-thick deposited layer, as shown in Fig. 3(b). The specimen also has a 2-mm-deep V-notch following the ASTM E23 standard. In high-pressure pressing dies, cracks initiate from the cavity surface and propagate inside the dies. Considering the characteristics of initiation and propagation of cracks in high-pressure tools, the V-notch was cut on the deposited region of the specimen. The impact test was performed at room temperature by using a Charpy impact machine, and the impact energy, impact velocity, and impact angle were set to 50 J, 3.8 m/s, and 150°, respectively. The impact absorption energy was calculated after the impact test, and the morphology of the fracture surface was examined using an FE-SEM.

3. RESULTS AND DISCUSSION

3.1. Microstructure

SEM micrographs (Figs. 4(a) and (b)) of the specimens showed that both H13 tool steel and M2 high-speed tool steel were successfully deposited on the D2 substrate. Sound

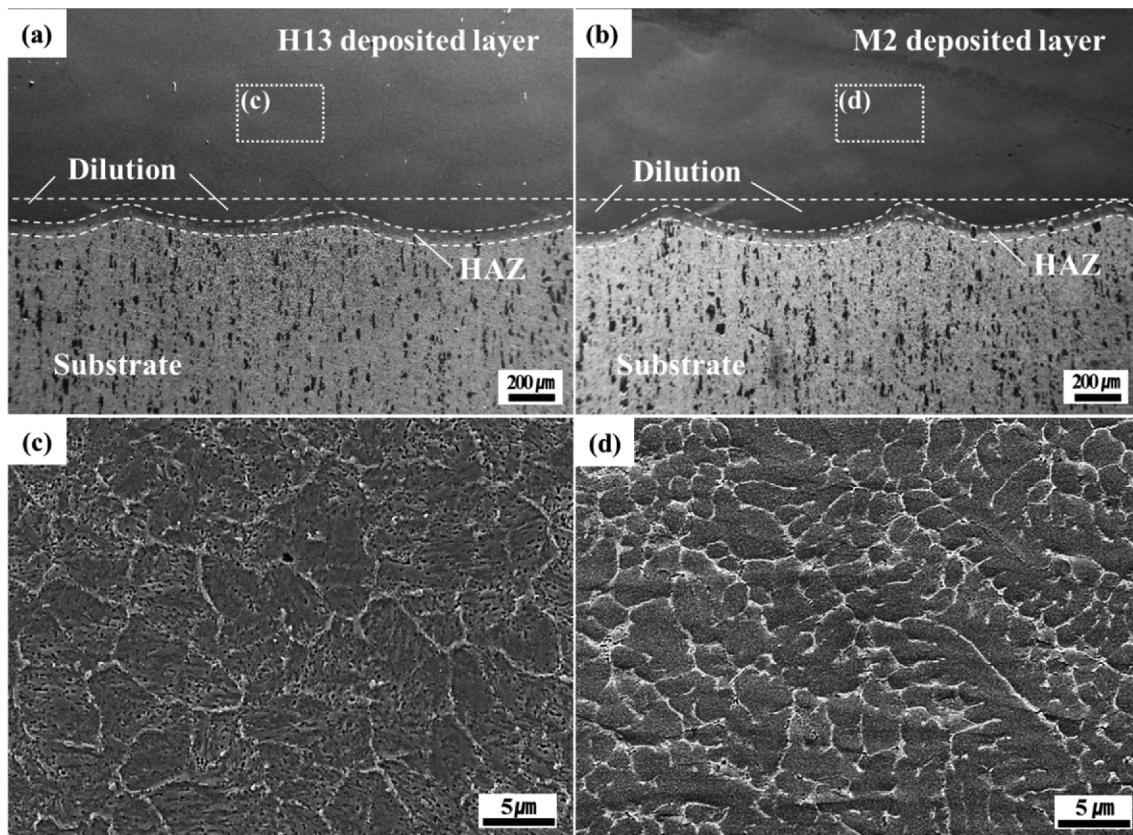


Fig. 4. SEM micrographs of deposited layer: (a) deposited H13 and substrate, (b) deposited M2 and substrate, (c) microstructure of deposited H13, and (d) microstructure of deposited M2.

interfaces without cracks or pores assured that there was a good bond between the deposits and the substrate.

The deposited specimens consist of the deposited layer, dilution, and heat affected zone (HAZ). It also can be seen that a wavy boundary line appears between each layer in the deposited layer as a result of re-melting. In the D2 substrate region, large and small carbides were dispersed in the ferrite matrix in the vertical direction. According to energy dispersive x-ray spectroscopy (EDS) analysis, the main ingredient of the carbides was found to be chrome. In the deposited layer, a dendritic structure, which resulted from melting by high-energy laser and rapid cooling, appeared in both the M2 and H13 deposits as depicted in Figs. 4(c) and 4(d). Figure 4(c) shows the microstructure at the central region of the deposited H13 layer, and fine cellular-dendrite (including fine carbides), retained austenite, and low carbon martensite are visible. The martensite formed during the fast solidification process after laser irradiation. During the solidification, primary austenite grows in the dendritic structure, and then transforms into martensite by rapid cooling. The microstructure of H13 is characterized by lath martensite with high dislocation density, vanadium-rich MC carbide, molybdenum-rich M_6C and M_2C carbides and chromium-rich M_7C_3 and $M_{23}C_6$ carbides, which also reported in the previous research [14]. In the deposited M2 layer as shown in Fig. 4(d), fine cellular-dendritic solidification structure is also shown as in the H13 microstructure. The main ingredients of the deposited dendritic structure were MC and M_6C , and the particles in the cells were found to be mainly M_6C carbide. The cellular grains of the deposited M2 layer were smaller than those of the H13 structure, which might result in higher hardness.

3.2. Microhardness

Figure 5 shows a macro-image of the M2 deposited specimen, and the hardness distributions in the horizontal and vertical directions over the deposited layer are shown in Fig. 6. Figure 6(a) shows the distribution of microhardness in the horizontal direction at positions 0.5 mm below the top surface of the deposited layer. The hardness of the substrate was shown to have an average of 200 Hv, and that of the heat-

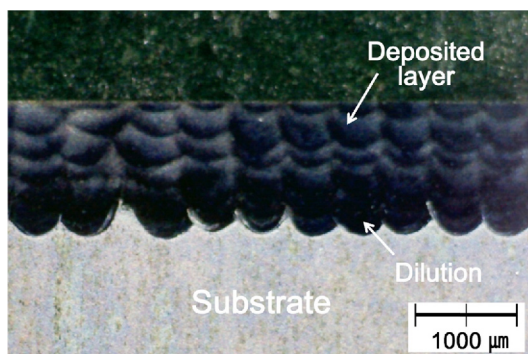


Fig. 5. Cross section of M2-deposited specimen.

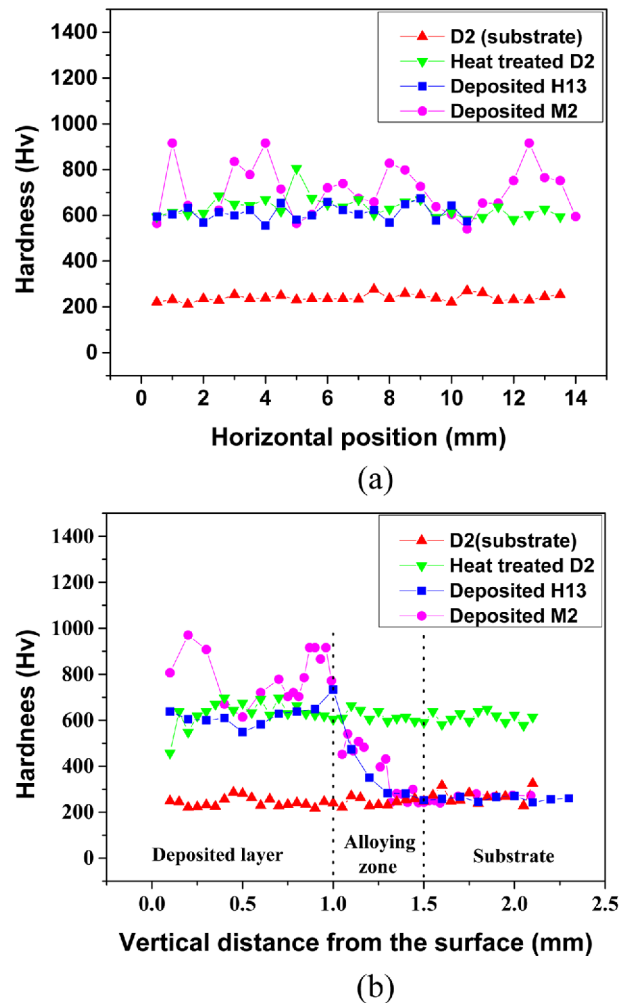


Fig. 6. Micro-hardness profiles in (a) horizontal direction and (b) vertical direction.

treated D2 was shown to have an average of 600 Hv, which was approximately 400 Hv higher than that of the substrate. The deposited H13 layer had an average hardness of 600 Hv, which is similar to that of the heat-treated D2, although its carbon content was smaller than that of D2. This is attributed to the microstructure refinement, martensite, and precipitated carbides resulting from the heating caused by the high power laser and the subsequent rapid cooling. The hardness of the deposited M2 metal powder layer was the highest, with an average value of 800 Hv, which suggests that the DED-based M2 hardfacing results in a significant improvement in the hardness of the deposited zone as compared to that of the heat-treated D2 substrate. This could be due to the hard elements, such as V and W, contained in M2 as well as the presence of martensite laths and precipitated carbides.

Figure 6(b) illustrates the microhardness variation with the depth from the top surface of the tool steel. D2 and the heat-treated D2 show uniform average hardness values of 200 Hv and 600 Hv, respectively. The H13 tool steel and the M2 high-

speed tool steel deposited layers differ in hardness depending on the location. In the deposited region, the hardness is uniform. The small range of variation at each location could be attributed to irregular powdered material flow (because of difficulties involved with powder mass flow control) and laser power fluctuation (because of thermal and optical instability during laser radiation). In some cases, the irregular dispersion of the carbides in the deposited region might be the cause of the hardness variation at each location. In addition, the hardness decreases in the alloying zone, where the depositing tool steel and the substrate were melted and mixed together in the melting pool; namely, the hardness decreased with the increase in the content of the substrate material. The subsequent gradual decrease in hardness in the interface between the alloying zone and the substrate is attributed to different amounts of tempering effect at different depths.

3.3. Wear Properties

During the wear test, a wear track appeared on all the specimens, caused by mechanical actions between the surfaces of the ball and the tested material, as shown in Fig. 7(a). The wear track of the heat-treated D2 formed a wear width of 1.23 mm, as shown in Fig. 7(b). Figure 7(c) shows the wear track of the H13-deposited specimen, of which the wear width is 1.82 mm, and there was more removal of the material from the deposited surface than for the heat-treated D2 surface. In the wear track of the M2-deposited specimen (Fig. 7(d)), the wear width was found to be the narrowest, showing a width of approximately 1.02 mm.

Figure 8 depicts the wear related results of each specimen.

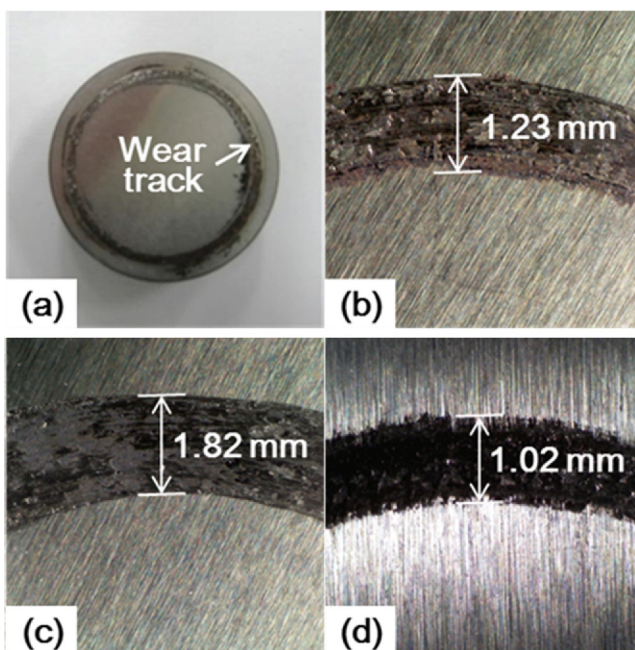


Fig. 7. (a) Macro image of worn track wear scar of (b) heat-treated D2, (c) deposited H13, and (d) deposited M2.

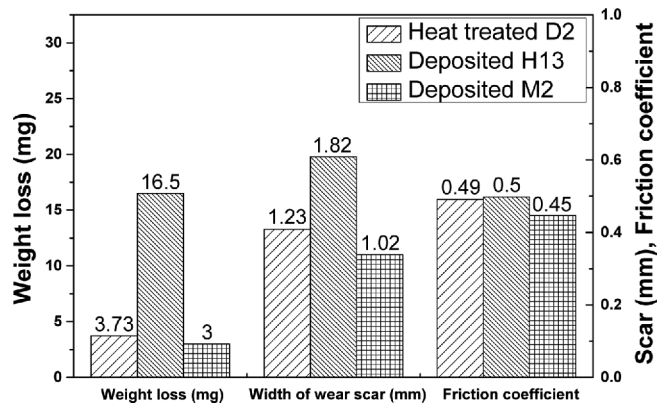


Fig. 8. Comparison of weight loss, width of wear scar, and friction coefficient of each specimen.

The weight reduction of the heat-treated D2 was 3.73 mg and the wear coefficient was found to be 0.49. The H13-deposited specimen, which formed the largest wear track width, experienced a weight reduction of 16.5 mg and a wear coefficient of 0.5; in turn, its wear resistance is most vulnerable among the tested specimens. In contrast, the M2-deposited specimen, which had the narrowest wear track width, underwent a weight reduction of only 3 mg, resulting in a wear coefficient of 0.45, which was the highest abrasive wear resistance among the tested materials. This result is attributed to the fact that the M2 alloy contains large amounts of hard-natured elements that can form carbides with vanadium, molybdenum, and tungsten. For tool steels containing a significant proportion of alloying elements and complex carbides, it was found that the wear resistance strongly depends on the proportion and type of the carbides [3]. The W- and Mo-rich carbides contained in the deposited H13 and M2 are harder and have higher wear resistance as compared with the Cr-rich carbides contained in the heat-treated D2 [15]. In addition, the V-rich carbides in the deposited M2 are harder and more wear-resistant than Mo- and W-rich carbides. Therefore, no significant scratching can be seen on the wear scar of the M2-deposited specimen. The aforementioned results indicate that the hardness is at least consistent with the wear resistance among the tested materials.

3.4. Impact Test

Resulting from the Charpy impact test, cracks initiated at the notch and propagated to the substrate for all tested specimens. As no cracks propagated through the interface between the deposited layer and the substrate (Figs. 9(a) and (b)), it is concluded that the deposit-substrate interface has good bonding strength.

Fracture morphologies are shown in Fig. 10. On the fracture surface of the heat-treated D2, transgranular fracture—where the fracture cracks pass through the grains—and micro void formation and coalescence (MVC), which is indicative

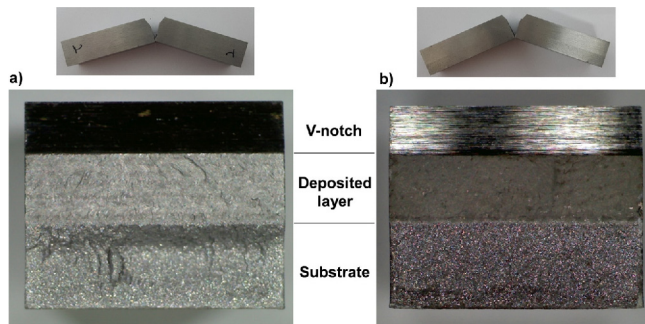


Fig. 9. Fractured specimens after Charpy test: (a) deposited H13 and (b) deposited M2.

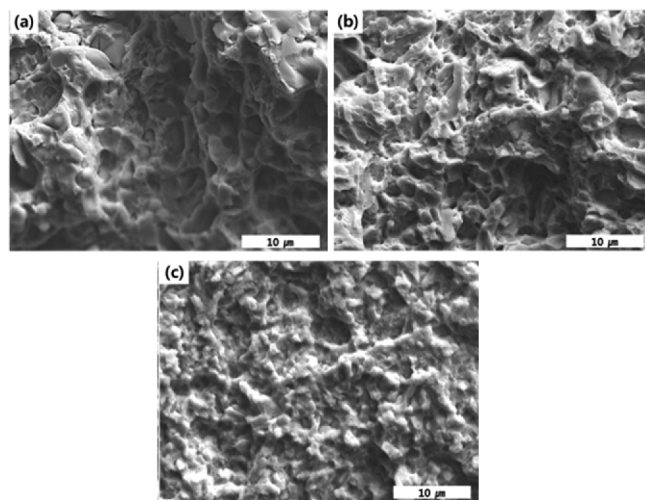


Fig. 10. SEM micrographs of fracture surface: (a) heat-treated D2, (b) deposited H13, and (c) deposited M2.

of localized ductile fracture, were observed as shown in Fig. 10(a). Figure 10(b) shows the fracture surface of the H13-deposited specimen, on which both transgranular and ductile fracture were observed simultaneously, similar to the fracture surface of the heat-treated D2. The void, or dimple mechanism was observed in two of the specimens (heat-treated D2 and deposited H13) but the dimple size was smaller in the H13 specimen than in the D2 specimen. Many tiny dimples—approximately 1 μm in size—appeared in the H13 fracture surface. Such fracture surfaces are quasi-cleavage faces that are generally observed in a tempered martensite microstructure. The micro voids are generated as a result of plastic deformation that is caused by inclusions smaller than 1 μm , such as oxides, carbides, and nitrides, existing in the material. Figure 10(c) shows the fracture surface of the M2-deposited specimen. The fracture surface is indicative of a typical brittle fracture (intergranular fracture) with no plastic deformation.

The total absorption energy of the heat-treated D2 specimen, H13-deposited specimen, and M2-deposited specimen were shown to be 1.425 J, 3.3017 J, and 0.98 J, respectively. The total absorption energy of the H13-deposited specimen,

which showed tiny dimples and a quasi-cleavage fracture surface, was highest. In contrast, the total absorption energy of the M2-deposited specimen, which showed intergranular fracture surface without plastic deformation, was lowest. Correspondingly, the fracture toughness of the H13-deposited specimen was found to be most superior, and the fracture toughness of the M2-deposited specimen, of which the hardness and wear resistance were superior, was shown to be relatively low. Nevertheless, the results of sound bond strength with no crack propagation through the interface between the deposited tool steels and the D2 substrate have demonstrated that hardfaced dies with deposited tool steels could successfully be applied to cold press dies/molds for fabrication of AHSS products.

4. CONCLUSION

In this study, H13 tool steel and M2 high-speed tool steel were deposited onto the surface of D2, which is widely used as a material for cold press dies/molds, with the purpose of possible hardfacing. To compare the mechanical properties of the deposited tool steels with the reference material (D2 prehardened by heat treatment), the micro-indentation test, wear test, and Charpy impact test were performed, and the following conclusions were drawn:

(1) Regarding the microstructure of the deposited layer, fine cellular-dendritic solidification structures resulting from melting and cooling were formed. The refined microstructure indicates that the deposited material experiences relatively rapid solidification during deposition, which could be effective in enhancing the resultant mechanical properties of the deposited material. The smaller cellular grains and precipitated carbides in the M2-deposited specimen led to the most enhanced hardness.

(2) The hardness and wear resistance of the M2-deposited specimen was found to be most superior, and the H13-deposited specimen showed hardness similar to that of the heat-treated D2. In the wear track of the deposited H13 layer, more material was removed from the H13-deposited surface than from the other wear tracks.

(3) Regarding the impact test, the H13-deposited specimen showed quasi-cleavage fracture morphology along with many tiny dimples, such that its total absorption energy was the highest among the tested specimens. In contrast, the M2-deposited specimen, with high hardness and great wear resistance, showed typical brittle fracture and was found to have relatively low fracture toughness in comparison to that of the H13-deposited specimen and the heat-treated D2. However, no crack propagated along the interface between the deposit and the substrate, which means that good bonding was achieved at the interface.

In this study, the mechanical properties of the M2 and H13 tool steels, which can be applied to the hardfacing of dies/

molds for cold pressing processes, were studied. The deposited H13 layer is expected to be effective in a forming die that requires high toughness. In contrast, the deposited M2 layer is expected to be effective in a blanking or piercing process that requires high wear resistance, as it exhibits high hardness and high wear resistance. However, when M2 powder is applied to a die to be used in a harsh environment, the relatively low toughness must be improved. For this reason, methods for enhancing the ductility, such as pre- or post- heat treatment, will be explored in the near future. In addition, the application of dissimilar powders mixed with a ductile material is worth studying.

ACKNOWLEDGEMENT

This work is supported by the Korea Institute of Industrial Technology (KITECH) under Grant Number EO17412 and by the Ministry of Strategy and Finance (MOSF). The authors express their sincere gratitude to the MOSF for providing financial support.

REFERENCES

1. S. D. Sun, Q. Liu, M. Brandt, V. Luzin, R. Cottam, M. Janardhana, *et al. Mat. Sci. Eng. A* **606**, 46 (2014).
2. N.-R. Park and D.-G. Ahn, *Int. J. Precis. Eng. Man.* **15**, 2549 (2014).
3. S. H. Wang, J.-Y. Chen, and L. Xue, *Surf. Coat. Technol.* **200**, 3446 (2006).
4. J. S. Park, M.-G. Lee, Y.-J. Cho, J. H. Sung, M.-S. Jeong, D. H. Kim, *et al. Met. Mater. Int.* **22**, 143 (2016).
5. M. Pleterski, T. Muhič, B. Podgornik, and J. Tušek, *Eng. Fail. Anal.* **18**, 1527 (2011).
6. D. Boisselier and S. Sankaré, *Phys. Procedia.* **39**, 455 (2012).
7. Y. Chew and J. H. L. Pang, *Int. J. Fatigue* **87**, 235 (2016).
8. J. H. Jang, B. D. Joo, S. M. Mun, M. Y. Sung, and Y. H. Moon, *Met. Mater. Int.* **17**, 167 (2011).
9. J. S. Kim, C.-M. Chung, S.-H. Baik, and S.-B. Lee, *Met. Mater. Int.* **17**, 77 (2011).
10. D. Das, R. Sarkar, A. K. Dutta, and K. K. Ray, *Mat. Sci. Eng. A* **528**, 589 (2010).
11. D. Cong, H. Zhou, Z. Ren, Z. Zhang, H. Zhang, C. Meng, *et al. Mater. Design* **55**, 597 (2014).
12. J. M. Torralba, L. E. G. Cambroner, J. M. Ruiz-Prieto, and M. M. das Neves, *Powder Metall.* **36**, 55 (1993).
13. C.-M. Kwon, G.-G. Lee, and G.-H. Ha, *Korean J. Met. Mater.* **54**, 10 (2016).
14. A. Medvedeva, J. Bergström, S. Gunnarsson, and J. Andersson, *Mat. Sci. Eng. A* **523**, 39 (2009).
15. S.-W. Choi, K.-H. Lee, J. Suh, M.-H. Oh, and C.-Y. Kang, *Korean J. Met. Mater.* **54**, 3 (2016).